

6

Electric and Magnetic Field Lenses

The subject of charged particle optics is introduced in this chapter. The concern is the control of the transverse motion of particles by shaped electric and magnetic fields. These fields bend charged particle orbits in a manner analogous to the bending of light rays by shaped glass lenses. Similar equations can be used to describe both processes. Charged particle lenses have extensive applications in such areas as electron microscopy, cathode ray tubes, and accelerator transport.

In many practical cases, beam particles have small velocity perpendicular to the main direction of motion. Also, it is often permissible to use special forms for the electric and magnetic fields near the beam axis. With these approximations, the transverse forces acting on particles are linear; they increase proportional to distance from the axis. The treatment in this chapter assumes such forces. This area is called *linear* or *Gaussian* charged particle optics.

Sections 6.2 and 6.3 derive electric and magnetic field expressions close to the axis and prove that any region of linear transverse forces acts as a lens. Quantities that characterize thick lenses are reviewed in Section 6.4 along with the equations that describe image formation. The bulk of the chapter treats a variety of static electric and magnetic field focusing devices that are commonly used for accelerator applications.

6.1 TRANSVERSE BEAM CONTROL

Particles in beams always have components of velocity perpendicular to the main direction of motion. These components can arise in the injector; charged particle sources usually operate at high temperature so that extracted particles have random thermal motions. In addition, the fields in injectors may have imperfections of shape. After extraction, space charge repulsion can accelerate particles away from the axis. These effects contribute to expansion of the beam. Accelerators and transport systems have limited transverse dimensions. Forces must be applied to deflect particles back to the axis. In this chapter, the problem of confining beams about the axis will be treated. When accelerating fields have a time dependence, it is also necessary to consider longitudinal confinement of particles to regions along the axis. This problem will be treated in Chapter 13.

Charged particle lenses perform three types of operations. One purpose of lenses is to *confine* a beam, or maintain a constant or slowly varying radius (see Fig. 6.1a). This is important in high-energy accelerators where particles must travel long distances through a small bore. Velocity spreads and space-charge repulsion act to increase the beam radius. Expansion can be countered

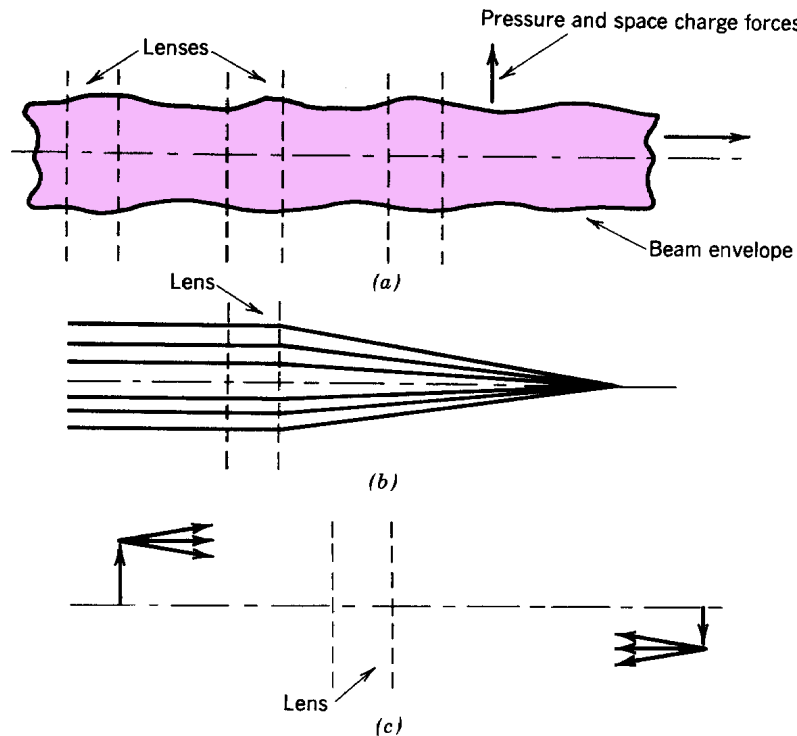


Figure 6.1 Functions of charged particle lenses. (a) Beam confinement. (b) Focusing to a spot. (c) Imaging.

Electric and Magnetic Field Lenses

by continuous confining forces which balance the outward forces or through a periodic array of lenses which deflect the particles toward the axis. In the latter case, the beam outer radius (or envelope) oscillates about a constant value.

A second function of lenses is to *focus* beams or compress them to the smallest possible radius (Fig. 6.1b). If the particles are initially parallel to the axis, a linear field lens aims them at a common point. Focusing leads to high particle flux or a highly localized beam spot. Focusing is important for applications such as scanning electron microscopy, ion microprobes, and ion-beam-induced inertial fusion.

A third use of charged particle lenses is forming an *image*. (Fig. 6.1c). When there is a spatial distribution of beam intensity in a plane, a lens can make a modified copy of the distribution in another plane along the direction of propagation. An image is formed if all particles that leave a point in one plane are mapped into another, regardless of their direction. An example of charged particle image formation is an image intensifier. The initial plane is a photo-cathode, where electrons are produced proportional to a light image. The electrons are accelerated and deflected by an electrostatic lens. The energetic electrons produce an enhanced copy of the light image when they strike a phosphor screen.

The terminology for these processes is not rigid. Transverse confinement is often referred to as focusing. An array of lenses that preserves the beam envelope may be called a focusing channel. The processes are, in a sense, interchangeable. Any linear field lens can perform all three functions.

6.2 PARAXIAL APPROXIMATION FOR ELECTRIC AND MAGNETIC FIELDS

Many particle beam applications require cylindrical beams. The electric and magnetic fields of lenses for cylindrical beams are azimuthally symmetric. In this section, analytic expressions are derived for such fields in the paraxial approximation. The term *paraxial* comes from the Greek *para* meaning "alongside of." Electric and magnetic fields are calculated at small radii with the assumption that the field vectors make small angles with the axis. The basis for the approximation is illustrated for a magnetic field in Figure 6.2. The currents that produce the field are outside the beam and vary slowly in z over scale lengths comparable to the beam radius.

Cylindrical symmetry allows only components B_r and B_z for static magnetic fields. Longitudinal currents at small radius are required to produce an azimuthal field B_θ . The assumptions of this section exclude both particle currents and displacement currents. Similarly, only the electric field components E_r and E_z are included. In the paraxial approximation, \mathbf{B} and \mathbf{E} make small angles with the axis so that $E_r \ll E_z$ and $B_r \ll B_z$.

Electric and Magnetic Field Lenses

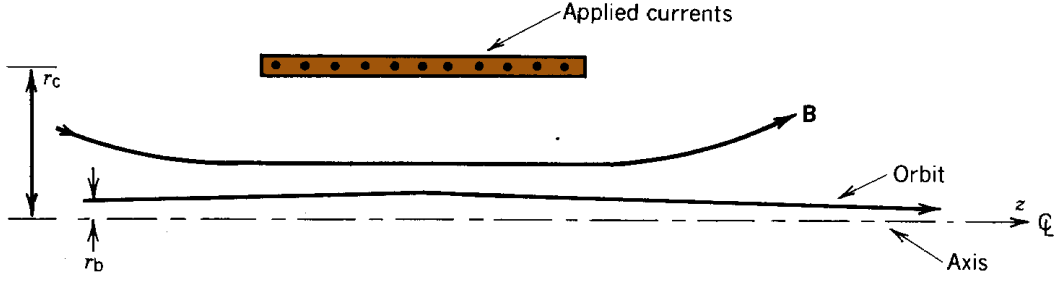


Figure 6.2 Validity conditions for the paraxial field approximation in a magnetic field lens.
Paraxial approximation: $r_b \ll r_c$; $v_r \ll v_z$; $B_r \ll B_z$.

The following form for electrostatic potential is useful to derive approximations for paraxial electric fields:

$$\begin{aligned} \varphi(r,z) = & \varphi(0,z) + Ar \left. \frac{\partial \varphi}{\partial z} \right|_o + Br^2 \left. \frac{\partial^2 \varphi}{\partial z^2} \right|_o \\ & + Cr^3 \left. \frac{\partial^3 \varphi}{\partial z^3} \right|_o + Dr^4 \left. \frac{\partial^4 \varphi}{\partial z^4} \right|_o + \dots \end{aligned} \quad (6.1)$$

The z derivatives of potential are evaluated on the axis. Note that Eq. (6.1) is an assumed form, not a Taylor expansion. The form is valid if there is a choice of the coefficients A, B, C, \dots , such that $\varphi(r, z)$ satisfies the Laplace equation in the paraxial approximation. The magnitude of terms decreases with increasing power of r . A term of order n has the magnitude $\varphi_o(\Delta r/\Delta z)^n$, where Δr and Δz are the radial and axial scale lengths over which the potential varies significantly. In the paraxial approximation, the quantity $\Delta r/\Delta z$ is small.

The electric field must go to zero at the axis since there is no included charge. This implies that $A = 0$ in Eq. (6.1). Substituting Eq. (6.1) into (4.19), we find that the coefficients of all odd powers of r must be zero. The coefficients of the even power terms are related by

$$\begin{aligned} & 4B \left. \frac{\partial^2 \varphi}{\partial z^2} \right|_o + 16D r^2 \left. \frac{\partial^4 \varphi}{\partial z^4} \right|_o \\ & + \dots + \left. \frac{\partial^2 \varphi}{\partial z^2} \right|_o + B r^2 \left. \frac{\partial^4 \varphi}{\partial z^4} \right|_o + \dots = 0. \end{aligned} \quad (6.2)$$

This is consistent if $B = -1/4$ and $D = -B/16 = 1/64$. To second order in $\Delta r/\Delta z$, $\varphi(r, z)$ can be expressed in terms of derivatives evaluated on axis by

$$\varphi(r,z) \cong \varphi(0,z) - (r^2/4) \left. \frac{\partial^2 \varphi}{\partial z^2} \right|_o. \quad (6.3)$$

The axial and radial fields are

$$E(0,z) \cong -\left. \frac{\partial \varphi}{\partial z} \right|_o, \quad E_r(r,z) \cong (r/2) \left. \frac{\partial^2 \varphi}{\partial z^2} \right|_o. \quad (6.4)$$

Electric and Magnetic Field Lenses

This gives the useful result that the radial electric field can be expressed as the derivative of the longitudinal field on axis:

$$E_r(r,z) \cong -(r/2) [\partial E_z(0,z)/\partial z]. \quad (6.5)$$

Equation (6.5) will be applied in deriving the paraxial orbit equation (Chapter 7). This equation makes it possible to determine charged particle trajectories in cylindrically symmetric fields in terms of field quantities evaluated on the axis. A major implication of Eq. (6.5) is that all transverse forces are linear in the paraxial approximation. Finally, Eq. (6.5) can be used to determine the radial variation of E_z . Combining Eq. (6.5) with the azimuthal curl equation ($\partial E_z/\partial r - \partial E_r/\partial z = 0$) gives

$$E_z(r,z) \cong E_z(0,z) - (r^2/4) [\partial^2 E_z(0,z)/\partial z^2]. \quad (6.6)$$

The variation of E_z is second order with radius. In the paraxial approximation, the longitudinal field and electrostatic potential are taken as constant in a plane perpendicular to the axis. A parallel treatment using the magnetic potential shows that

$$B_r(r,z) \cong -(r/2) [\partial B_z(0,z)/\partial z]. \quad (6.7)$$

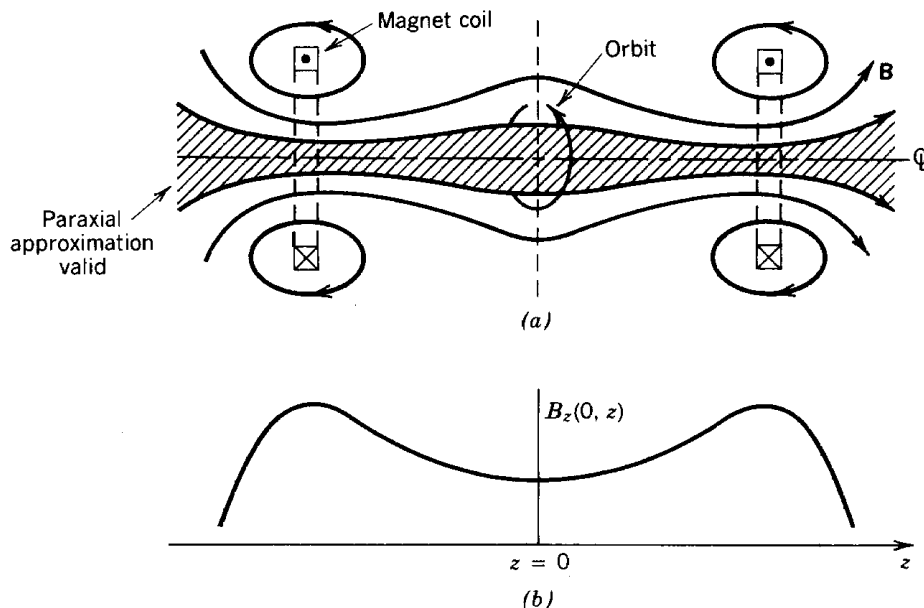


Figure 6.3 Magnetic mirror field. (a) Geometry, field components, and forces on a particle with an axi-centered orbit. (b) Variation of axial field on-axis, $B_z(0, z)$.

Electric and Magnetic Field Lenses

Figure 6.3 is an example of a paraxial magnetic field distribution. The fields are produced by two axicentered circular coils with currents in the same direction. In plasma research, the field distribution is called a *magnetic mirror*. It is related to the fields used in cyclotrons and betatrons. The magnitude of $B_z(0, z)$ is maximum at the coils. The derivative of B_z is positive for $z > 0$ and negative for $z < 0$. Consider a positively charged particle with an axicentered circular orbit that has a positive azimuthal velocity. If the particle is not midway between the coils, there will be an axial force $qv_\theta B_r$. Equation (6.7) implies that this force is in the negative z direction for $z > 0$ and the converse when $z < 0$. A magnetic mirror can provide radial and axial confinement of rotating charged particles. An equivalent form of Eq. (6.6) holds for magnetic fields. Because $\partial B_z^2 / \partial z^2$ is positive in the mirror, the magnitude of B_z decreases with radius.

6.3 FOCUSING PROPERTIES OF LINEAR FIELDS

In this section, we shall derive the fact that all transverse forces that vary linearly away from an axis can focus a parallel beam of particles to a common point on the axis. The parallel beam, shown in Figure 6.4, is a special case of *laminar* motion. Laminar flow (from *lamina*, or layer) implies that particle orbits at different radii follow streamlines and do not cross. The ideal laminar beam has no spread of transverse velocities. Such beams cannot be produced, but in many cases laminar motion is a valid first approximation. The derivation in this section also shows that linear forces preserve laminar flow.

The radial force on particles is taken as $F_r(r) = -A(z, v_r) r$. Section 6.2 showed that paraxial electric forces obey this equation. It is not evident that magnetic forces are linear with radius since particles can gain azimuthal velocity passing through radial magnetic fields. The proof that the

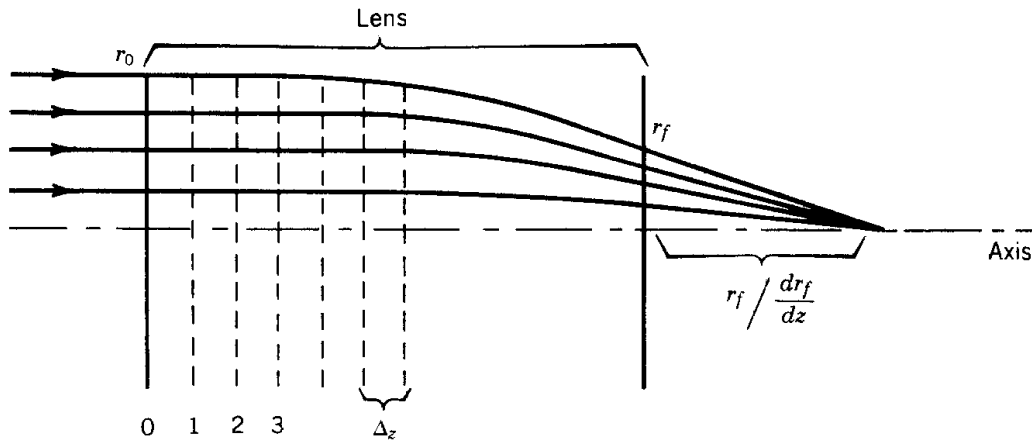


Figure 6.4 Finite difference calculation of the effect of linear focusing fields on particle orbits.

Electric and Magnetic Field Lenses

combination of magnetic and centrifugal forces gives a linear radial force variation is deferred to Section 6.7.

Particle orbits are assumed paraxial; they make small angles with the axis. This means that $v_r \ll v_z$. The total velocity of a particle is $v_o^2 = v_r^2 + v_z^2$. If v_o is constant, changes of axial velocity are related to changes of radial velocity by

$$\Delta v_z/v_z \cong -(v_r/v_z) (\Delta v_r/v_z).$$

Relative changes of axial velocity are proportional to the product of two small quantities in the paraxial approximation. Therefore, the quantity v_z is almost constant in planes normal to z . The average axial velocity may vary with z because of acceleration in E_z fields. If v_z is independent of r , time derivatives can be converted to spatial derivatives according to

$$d/dt \Rightarrow v_z (d/dz). \quad (6.8)$$

The interpretation of Eq. (6.8) is that the transverse impulse on a particle in a time Δt is the same as that received passing through a length element $\Delta z = v_z \Delta t$. This replacement gives differential equations expressing radius as a function of z rather than t . In treatments of steady-state beams, the orbits $r(z)$ are usually of more interest than the instantaneous position of any particle.

Consider, for example, the nonrelativistic transverse equation of motion for a particle moving in a plane passing through the axis in the presence of azimuthally symmetric radial forces

$$d^2 r/dt^2 = F_r(r, z, v_z)/m_o.$$

Converting time derivatives to axial derivatives according to Eq. 6.8 yields

$$d(v_z r')/dt = v_z r' v_z' + v_z^2 r'' = F_r/m_o,$$

or

$$dr'/dz = F_r(r, z, v_z)/m_o v_z^2 - v_z' r'/v_z, \quad r' = dr/dz. \quad (6.9)$$

A primed quantity denotes an axial derivative. The quantity r' is the angle between the particle orbit and the axis. The motion of a charged particle through a lens can be determined by a numerical solution of Eqs. (6.9). Assume that the particle has $r = r_o$ and $r' = 0$ at the lens entrance. Calculation of the final position, r_f and angle, r_f' determines the focal properties of the fields. Further, assume that F_r is linear and that $v_z(0, z)$ is a known function calculated from $E_z(0, z)$. The region over which lens forces extend is divided into a number of elements of length Δz . The following numerical algorithm (the *Eulerian difference method*) can be used to find a

Electric and Magnetic Field Lenses

particle orbit.

$$\begin{aligned}
 r(z+\Delta z) &= r(z) + r'(z)\Delta z, \\
 r'(z+\Delta z) &= r'(z) - [A(z, v_z)r/m_o v_z^2 + v_z' r'/v_z]\Delta z \\
 r'(z) &= [a_1(z)r + a_2(z)r'] \Delta z.
 \end{aligned} \tag{6.10}$$

More accurate difference methods will be discussed in Section 7.8.

Applying Eq. (6.10), position and velocity at the first three positions in the lens are

$$\begin{aligned}
 r_o &= r_o, \quad r_o' = 0, \\
 r_1 &= r_o, \quad r_1' = -a_1(0)r_o\Delta z, \\
 r_2 &= r_o - a_1(0)r_o, \\
 r_2' &= -a_1(0)r_o\Delta z - a_1(\Delta z)r_o\Delta z + a_2(\Delta z)a_1(0)r_o\Delta z.
 \end{aligned} \tag{6.11}$$

Note that the quantity r_o appears in all terms; therefore, the position and angle are proportional to r_o at the three axial locations. By induction, this conclusion holds for the final position and angle, r_f and r_f' . Although the final orbit parameters are the sum of a large number of terms (becoming infinite as Δz approaches zero), each term involves a factor of r_o . There are two major results of this observation.

1. The final radius is proportional to the initial radius for all particles. Therefore, orbits do not cross. A linear force preserves laminar motion.
2. The final angle is proportional to r_o ; therefore, r_f' is proportional to r_o . In the paraxial limit, the orbits of initially parallel particles exiting the lens form similar triangles. All particles pass through the axis at a point a distance r_f/r_f' from the lens exit (Fig. 6.4).

The conclusion is that any region of static, azimuthally symmetric electric fields acts as a lens in the paraxial approximation. If the radial force has the form $+A(z, v_z)r$, the final radial velocity is positive. In this case, particle orbits form similar triangles that emanate from a point upstream. The lens, in this case, is said to have a *negative focal length*.

6.4 LENS PROPERTIES

The lenses used in light optics can often be approximated as thin lenses. In the thin-lens

Electric and Magnetic Field Lenses

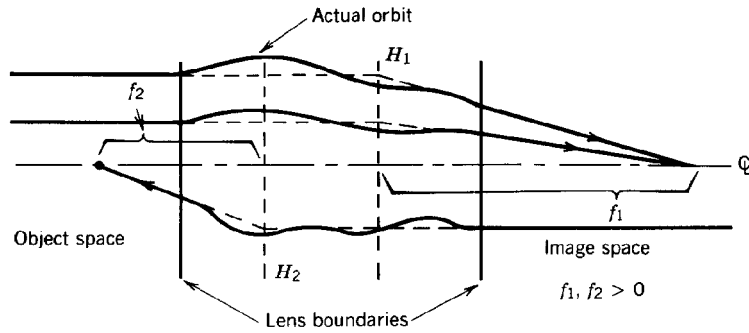


Figure 6.5 Charged particle lens. Definition of quantities used in linear approximation (Gaussian optics): principal planes (H_1, H_2) and focal lengths (f_1, f_2).

approximation, rays are deflected but have little change in radius passing through the lens. This approximation is often invalid for charged particle optics; the Laplace equation implies that electric and magnetic fields extend axial distances comparable to the diameter of the lens. The particle orbits of Figure 6.4 undergo a significant radius change in the field region. Lenses in which this occurs are called *thick lenses*. This section reviews the parameters and equations describing thick lenses.

A general charged particle lens is illustrated in Figure 6.5. It is an axial region of electric and magnetic fields that deflects (and may accelerate) particles. Particles drift in *ballistic orbits* (no acceleration) in field-free regions outside the lens. The upstream field-free region is called the *object space* and the downstream region is called the *image space*. Lenses function with particle motion in either direction, so that image and object spaces are interchangeable.

Orbits of initially parallel particles exiting the lens form similar triangles (Fig. 6.5). If the exit orbits are projected backward in a straight line, they intersect the forward projection of entrance orbits in a plane perpendicular to the axis. This is called the *principal plane*. The location of the principal plane is denoted H_j . The distance from H_1 to the point where orbits intersect is called the *focal length*, f_1 . When H_1 and f_1 are known, the exit orbit of any particle that enters the lens parallel to the axis can be specified. The exit orbit is the straight line connecting the focal point to the intersection of the initial orbit with the principal plane. This construction also holds for negative focal lengths, as shown in Figure 6.6.

There is also a principal plane (H_2) and focal length (f_2) for particles with negative v_z . The focal lengths need not be equal. This is often the case with electrostatic lenses where the direction determines if particles are accelerated or decelerated. Two examples of $f_1 \neq f_2$ are the aperture lens (Section 6.5) and the immersion lens (Section 6.6). A *thin lens* is defined as one where the axial length is small compared to the focal length. Since the principal planes are contained in the field region, $H_1 = H_2$. A thin lens has only one principal plane. Particles emerge at the same radius they entered but with a change in direction.

Electric and Magnetic Field Lenses

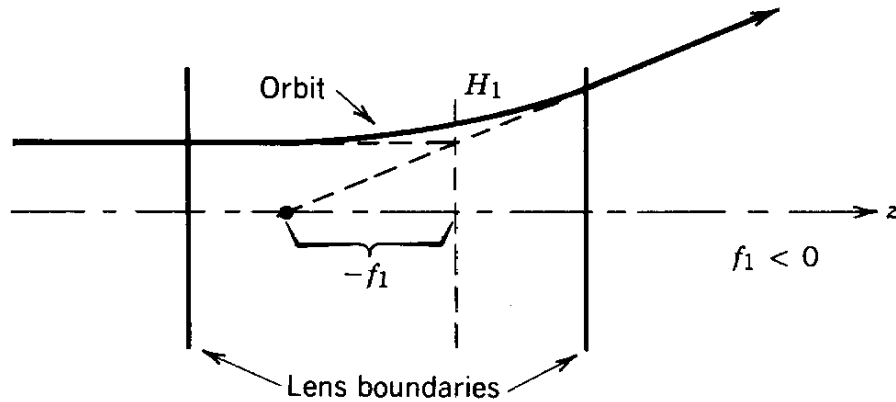


Figure 6.6 Construction of a particle orbit in a lens with a negative focal length.

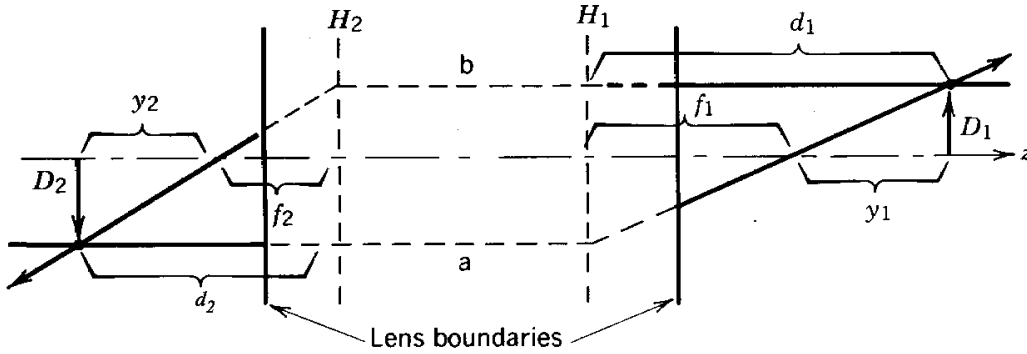
There are two other common terms applied to lenses, the lens power and the *f-number*. The strength of a lens is determined by how much it bends orbits. Shorter focal lengths mean stronger lenses. The lens power P is the inverse of the focal length, $P = 1/f$. If the focal length is measured in meters, the power is given in m^{-1} or *diopeters*. The *f-number* is the ratio of focal length to the lens diameter: $f\text{-number} = f/D$. The *f-number* is important for describing focusing of nonlaminar beams. It characterizes different optical systems in terms of the minimum focal spot size and maximum achievable particle flux.

If the principal planes and focal lengths of a lens are known, the transformation of an orbit between the lenses entrance and exit can be determined. This holds even for nonparallel entrance orbits. The conclusion follows from the fact that particle orbits are described by a linear, second-order differential equation. The relationship between initial and final orbits ($r_i, r_i' \Rightarrow r_f, r_f'$) can be expressed as two algebraic equations with four constant coefficients. Given the two initial conditions and the coefficients (equivalent to the two principal planes and focal lengths), the final orbit is determined. This statement will be proved in Chapter 8 using the ray transfer matrix formalism.

Chapter 8 also contains a proof that a linear lens can produce an image. The definition of an image is indicated in Figure 6.7. Two special planes are defined on either side of the lens: the *object plane* and the *image plane* (which depends on the lens properties and the location of the object). An image is produced if all particles that leave a point in the object plane meet at a point in the image plane, independent of their initial direction. There is a mapping of spatial points from one plane to another. The image space and object space are interchangeable, depending on the direction of the particles. The proof of the existence of an image is most easily performed with matrix algebra. Nonetheless, assuming this property, the principal plane construction gives the locations of image and object planes relative to the lens and the magnification passing from one to another.

Figure 6.7 shows image formation by a lens. Orbits in the image and object space are related by the principal plane construction; the exit orbits are determined by the principal plane and focal length. These quantities give no detailed information on orbits inside the lens. The arrows

Electric and Magnetic Field Lenses



(Actual orbits unspecified in this region)

Figure 6.7 Quantities for calculating the imaging properties of a thick lens.

represent an intensity distribution of particles in the transverse direction. Assume that each point on the source arrow (of length D_2) is mapped to a point in the image plane. The mapping produces an image arrow of length D_1 . Parallel orbits are laminar, and the distance from the axis to a point on the image is proportional to its position on the source. We want to find the locations of the image and object planes (d_1 and d_2) relative to the principal planes, as well as the magnification, $M_{21} = D_1/D_2$.

The image properties can be found by following two particle orbits leaving the object. Their intersection in the image space determines the location of the image plane. The orbit with known properties is the one that enters the lens parallel to the axis. If a parallel particle leaves the tip of the object arrow, it exits the lens following a path that passes through the intersection with the principal plane at $r = D_2$ and the point f_1 . This orbit is marked *a* in Figure 6.7. In order to determine a second orbit, we can interchange the roles of image and object and follow a parallel particle that leaves the right-hand arrow in the $-z$ direction. This orbit, marked *b*, is determined by the points at H_2 and f_2 . A property of particle dynamics under electric and magnetic forces is time reversibility. Particles move backward along the same trajectories if $-t$ is substituted for t . Thus, a particle traveling from the original object to the image plane may also follow orbit *b*. If the two arrows are in object and image planes, the orbits must connect as shown in Figure 6.7.

The image magnification for particles traveling from left to right is $M_{21} = D_1/D_2$. For motion in the opposite direction, the magnification is $M_{12} = D_2/D_1$. Therefore,

$$M_{21} M_{12} = 1. \quad (6.12)$$

Referring to Figure 6.7, the following equations follow from similar triangles:

$$D_1/y_1 = D_2/f_1, \quad D_1/f_2 = D_2/y_2. \quad (6.13)$$

Electric and Magnetic Field Lenses

These are combined to give $f_1 f_2 = y_1 y_2$. This equation can be rewritten in terms of the distances d_1 and d_2 from the principal planes as $f_1 f_2 = (d_2 - f_2)(d_1 - f_1)$. The result is the thick-lens equation

$$f_1/d_1 + f_2/d_2 = 1. \quad (6.14)$$

In light optics, the focal length of a simple lens does not depend on direction. In charged particle optics, this holds for magnetic lenses or *unipotential* electrostatic lenses where the particle energy does not change in the lens. In this case, Eq. (6.14) can be written in the familiar form

$$1/d_1 + 1/d_2 = 1/f, \quad (6.15)$$

where $f_1 = f_2 = f$.

In summary, the following procedure is followed to characterize a linear lens. Measured data or analytic expressions for the fields of the lens are used to calculate two special particle orbits. The orbits enter the lens parallel to the axis from opposite axial directions. The orbit calculations are performed analytically or numerically. They yield the principal planes and focal lengths. Alternately, if the fields are unknown, lens properties may be determined experimentally. Parallel particle beams are directed into the lens from opposite directions to determine the lens parameters. If the lens is linear, all other orbits and the imaging properties are found from two measurements.

In principle, the derivations of this section can be extended to more complex optical systems. The equivalent of Eq. (6.14) could be derived for combinations of lenses. On the other hand, it is much easier to treat optical systems using ray transfer matrices (Chapter 8). Remaining sections of this chapter are devoted to the calculation of optical parameters for a variety of discrete electrostatic and magnetostatic charged particle lenses.

6.5 ELECTROSTATIC APERTURE LENS

The electrostatic aperture lens is an axicentered hole in an electrode separating two regions of axial electric field. The lens is illustrated in Figure 6.8. The fields may be produced by grids with applied voltage relative to the aperture plate. If the upstream and downstream electric fields differ, there will be radial components of electric field near the hole which focus or defocus particles. In Figure 6.8, axial electric fields on both sides of the plate are positive, and the field at the left is stronger. In this case, the radial fields point outward and the focal length is negative for positively charged particles traveling in either direction. With reversed field direction (keeping the same relative field strength) or with stronger field on the right side (keeping the same field polarity), the lens has positive focal length. The transverse impulse on a particle passing through the hole is

Electric and Magnetic Field Lenses

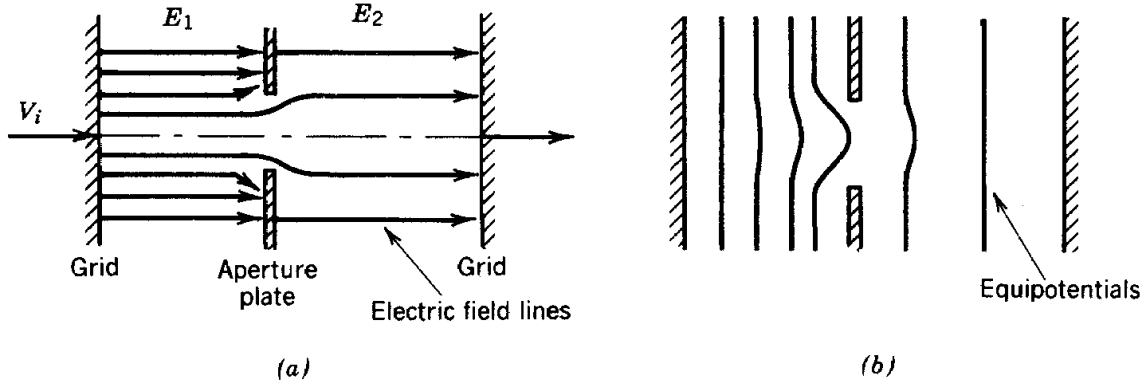


Figure 6.8 Electrostatic aperture lens. (a) Geometry, showing electric field lines. (b) Equipotential lines.

proportional to the time spent in the radial electric fields. This is inversely proportional to the particle velocity which is determined, in part, by the longitudinal fields. Furthermore, the final axial velocity will depend on the particle direction. These factors contribute to the fact that the focal length of the aperture lens depends on the transit direction of the particle, or $f_1 \neq f_2$.

Radial electric fields are localized at the aperture. Two assumptions allow a simple estimate of the focal length: (1) the relative change in radius passing through the aperture is small (or, the aperture is treated in the thin lens approximation) and (2) the relative change in axial velocity is small in the vicinity of the aperture. Consider a particle moving in the $+z$ direction with $v_r = 0$. The change in v_r for nonrelativistic motion is given by the equation

$$dv_r/dz = qE_r/m_o v_z \cong -(q/2m_o v_z) r [dE_z(0,z)/dz]. \quad (6.16)$$

In Eq. (6.16), the time derivative was converted to a spatial derivative and E_r was replaced according to Eq. (6.5).

With the assumption of constant r and v_z in the region of nonzero radial field, Eq. (6.16) can be integrated directly to yield

$$v_{rf} / v_{zf} = r_f' \cong -qr (E_{z2} - E_{z1})/2m_o v_{za} v_{zf} \quad (6.17)$$

where v_{za} is the particle velocity at the aperture and v_{rf} is the radial velocity after exiting. The quantity v_{zf} is the final axial velocity; it depends on the final location of the particle and the field E_{z2} . The focal length is related to the final radial position (r) and the ratio of the radial velocity to the final axial velocity by $v_{rf}/v_{zf} \approx r/f$. The focal length is

Electric and Magnetic Field Lenses

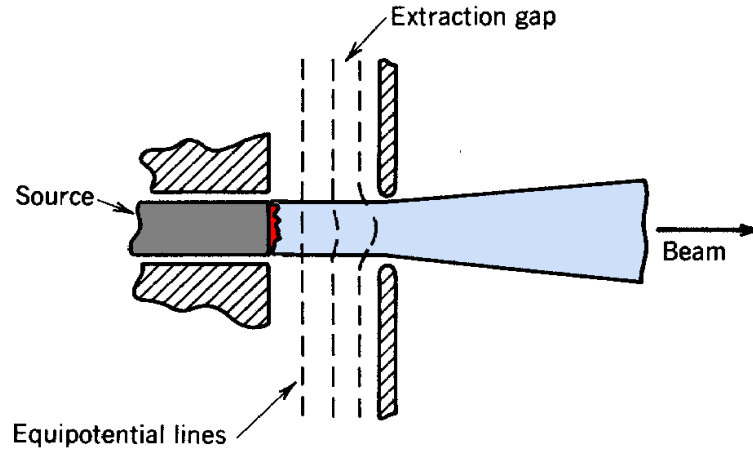


Figure 6.9 Extraction gap of an electron gun showing negative-lens effect.

$$f \cong 2m_o v_{za} v_{zf} / q (E_{z2} - E_{z1}). \quad (6.18)$$

When the particle kinetic energy is large compared to the energy change passing through the lens, $v_{za} \cong v_{zf}$, and we find the usual approximation for the aperture lens focal length

$$f \cong 2m_o v_{zf}^2 / q(E_{z2} - E_{z1}) = 4T/q(E_{z2} - E_{z1}). \quad (6.19)$$

The *charged particle extractor* (illustrated in Fig. 6.9) is a frequently encountered application of Eq. (6.19). The extractor gap pulls charged particles from a source and accelerates them. The goal is to form a well-directed low-energy beam. When there is high average beam flux, grids cannot be used at the downstream electrode and the particles must pass through a hole. The hole acts as an aperture lens, with $E_1 > 0$ and $E_2 = 0$. The focal length is negative; the beam emerging will diverge. This is called the *negative lens effect* in extractor design. If a parallel or focused beam is required, a focusing lens can be added downstream or the source can be constructed with a concave shape so that particle orbits converge approaching the aperture.

6.6 ELECTROSTATIC IMMERSION LENS

The geometry of the electrostatic immersion lens is shown in Figure 6.10. It consists of two tubes at different potential separated by a gap. Acceleration gaps between drift tubes of a standing-wave linear accelerator (Chapter 14) have this geometry. The one-dimensional version of this lens occurs in the gap between the Dees of a cyclotron (Chapter 15). Electric field distributions for a cylindrical lens are plotted in Figure 6.10.

Electric and Magnetic Field Lenses

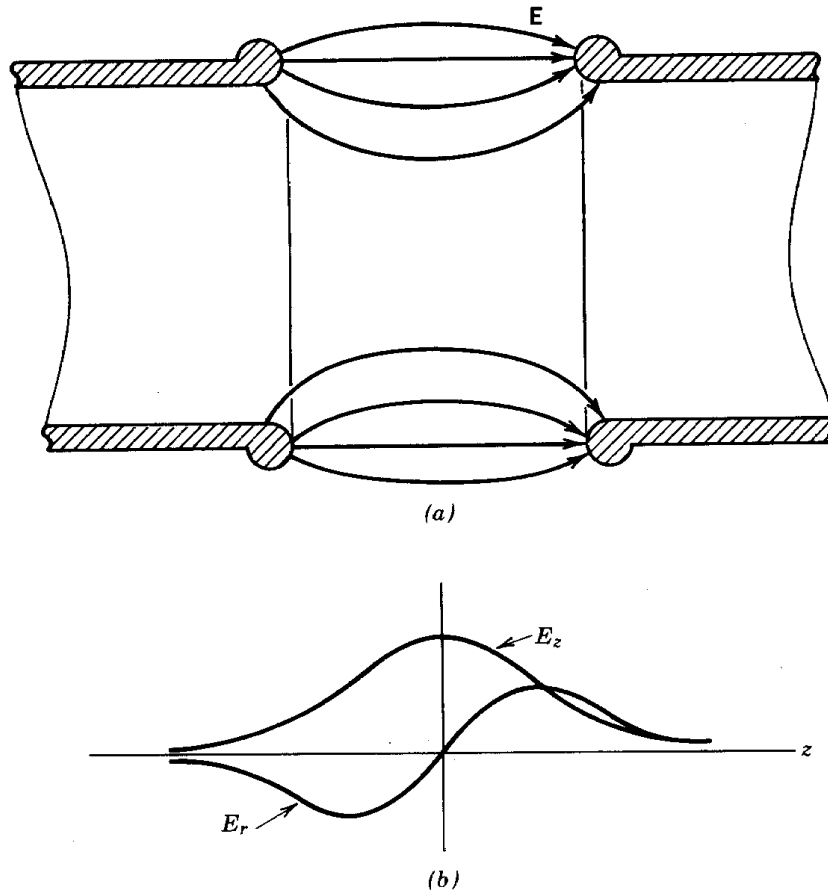


Figure 6.10 Electrostatic immersion lens. (a) Geometry and electric field lines. (b) Relative variations of longitudinal electric field, $E_z(0, z)$ (on-axis), and transverse field, $E_r(r, z)$ (off-axis), moving through the lens.

Following the treatment used for the aperture lens, the change in radial velocity of a particle passing through the gap is

$$\Delta v_r = v_{rf} = \int dz [qE_r(r,z)/m_o v_z]. \quad (6.20)$$

The radial electric field is symmetric. There is no deflection if the particle radius and axial velocity are constant. In contrast to the aperture lens, the focusing action of the immersion lens arises from changes in r and v_z in the gap region. Typical particle orbits are illustrated in Figure 6.11. When the longitudinal gap field accelerates particles, they are deflected inward on the entrance side of the lens and outward on the exit side. The outward impulse is smaller because (1) the particles are closer to the axis and (2) they move faster on the exit side. The converse holds for a decelerating gap. Particles are deflected to larger radii on the entrance side and are therefore more strongly influenced by the radial fields on the exit side. Furthermore, v_z is lower at the exit side enhancing

Electric and Magnetic Field Lenses

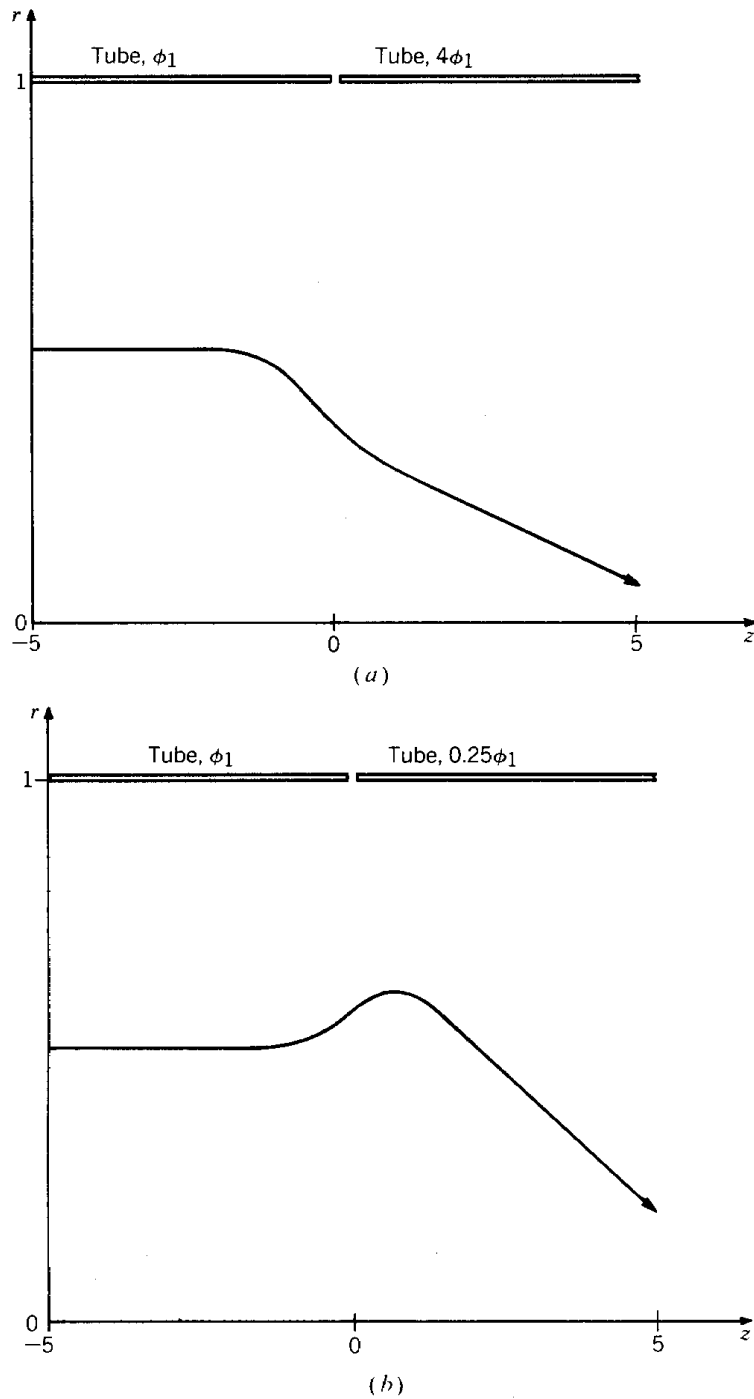


Figure 6.11 Particle trajectories in an immersion lens. (a) Accelerating lens (final kinetic energy equals 4 times initial energy). (b) Decelerating lens (final kinetic energy equals 0.25 times initial energy). (Note expanded radial scale).

Electric and Magnetic Field Lenses

focusing. The focal length for either polarity or charge sign is positive.

The orbits in the immersion lens are more complex than those in the aperture lens. The focal length must be calculated from analytic or numerical solutions for the electrostatic fields and numerical solutions of particle orbits in the gap. In the paraxial approximation, only two orbits need be found. The results of such calculations are shown in Figure 6.12 for varying tube diameter with a narrow gap. It is convenient to reference the tube potentials to the particle source so that the exit energy is given by $T_f = qV_2$. With this convention, the abscissa is the ratio of exit to entrance kinetic energy. The focal length is short (lens power high) when there is a significant change in kinetic energy passing through the lens. The *einzel lens* is a variant of the immersion lens often encountered in low-energy electron guns. It consists of three colinear tubes, with the middle tube elevated to high potential. The einzel lens consists of two immersion lenses in series; it is a unipotential lens.

An interesting modification of the immersion lens is *foil* or *grid focusing*. This focusing method, illustrated in Figure 6.13, has been used in low-energy linear ion accelerators. A conducting foil or mesh is placed across the downstream tube of an accelerating gap. The resulting field pattern looks like half of that for the immersion lens. Only the inward components of radial field are present. The paraxial approximation no longer applies; the foil geometry has first-order focusing. Net deflections do not depend on changes of r and v_z as in the immersion lens. Consequently, focusing is much stronger. Foil focusing demonstrates one of the advantages gained by locating charges and currents within the beam volume, rather than relying on external electrodes or coils.

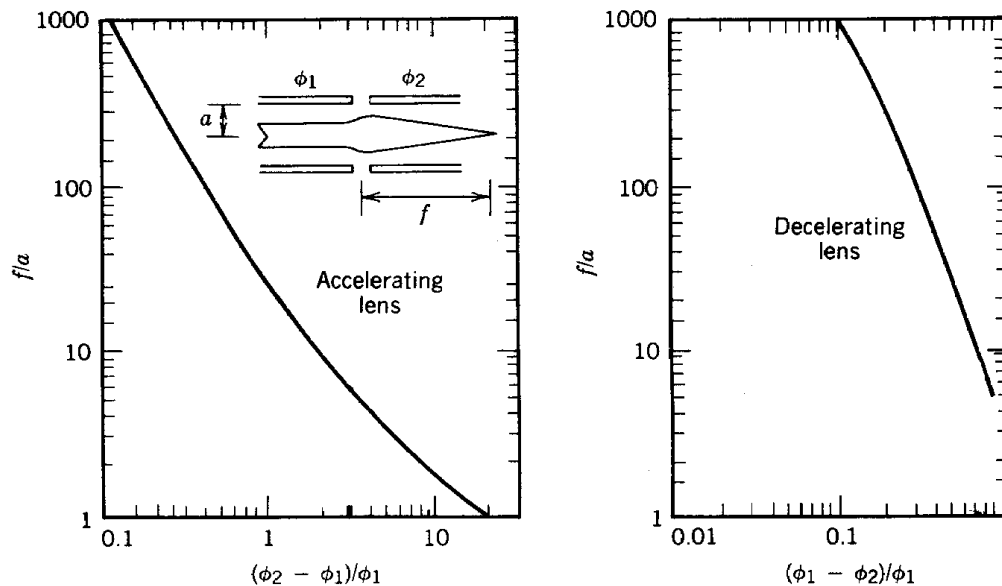


Figure 6.12 Focal lengths of immersion lenses in terms of relative kinetic energy change in lens. (a) Accelerating lenses. (b) Decelerating lenses.

Electric and Magnetic Field Lenses

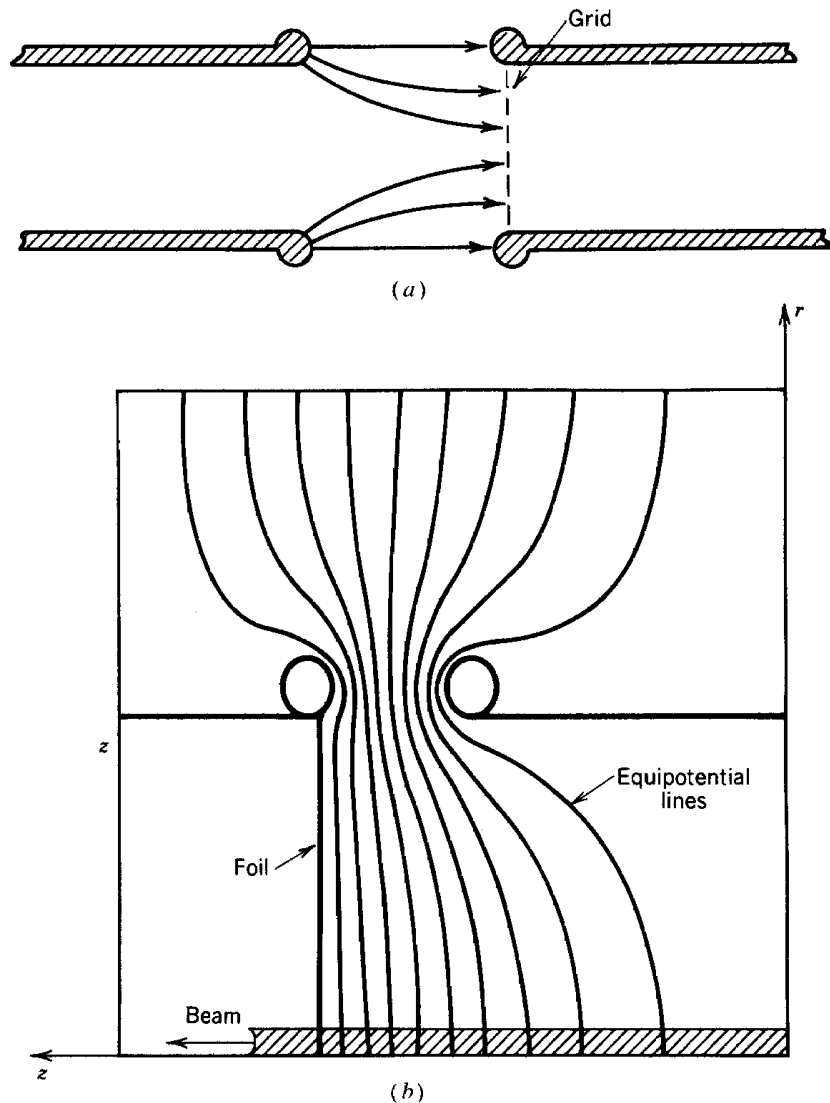


Figure 6.13 Accelerating gap of a drift tube linear accelerator with a grid for enhanced electrostatic focusing. (a) Geometry. (b) Equipotential lines.

The charges, in this case, are image charges on the foil. An example of internal currents, the toroidal field magnetic sector lens, is discussed in Section 6.8.

6.7 SOLENOIDAL MAGNETIC LENS

The *solenoidal magnetic lens* is illustrated in Figure 6.14. It consists of a region of cylindrically

Electric and Magnetic Field Lenses

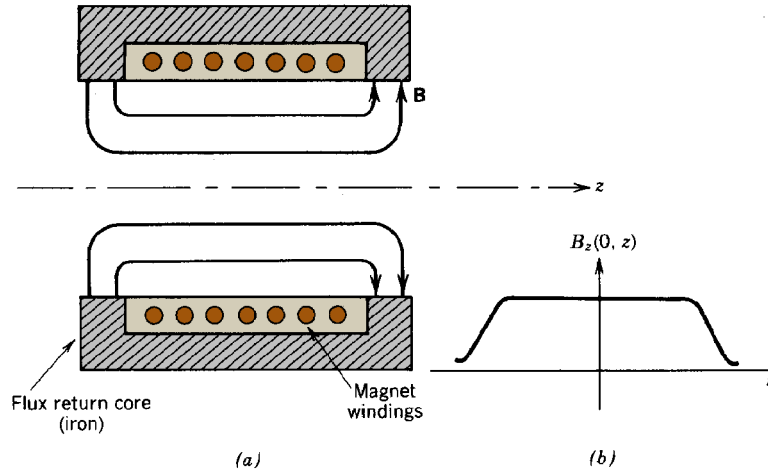


Figure 6.14 Solenoidal magnetic lens. (a) Geometry and field lines. (b) Variation of longitudinal magnetic field on axis, $B_z(0, z)$.

symmetric radial and axial magnetic fields produced by axicentered coils carrying azimuthal current. This lens is the only possible magnetic lens geometry consistent with cylindrical paraxial beams. It is best suited to electron focusing. It is used extensively in cathode ray tubes, image intensifiers, electron microscopes, and electron accelerators. Since the magnetic field is static, there is no change of particle energy passing through the lens; therefore, it is possible to perform relativistic derivations without complex mathematics.

Particles enter the lens through a region of radial magnetic fields. The Lorentz force ($ev_z \times B_r$) is azimuthal. The resulting v_θ leads to a radial force when crossed into the B_z fields inside the lens. The net effect is a deflection toward the axis, independent of charge state or transit direction. Because there is an azimuthal velocity, radial and axial force equations must be solved with the inclusion of centrifugal and coriolis forces.

The equations of motion (assuming constant γ) are

$$\gamma m_o (dv_r/dt) = -qv_\theta B_z + \gamma m_o v_\theta^2/r, \quad (6.21)$$

$$\gamma m_o (dv_\theta/dt) = -qv_z B_z - \gamma m_o v_r v_\theta/r. \quad (6.22)$$

The axial equation of motion is simply that v_z is constant. We assume that r is approximately constant and that the particle orbit has a small net rotation in the lens. With the latter condition, the Coriolis force can be neglected in Eq. (6.22). If the substitution $dv_\theta/dt \approx v_z (dv_\theta/dz)$ is made and Eq. (6.7) is used to express B_r in terms of $dB_z(0, z)/dz$, Eq. (6.22) can be integrated to give

$$v_\theta - qrB_z/2\gamma m_o = \text{constant} = 0. \quad (6.23)$$

Equation (6.23) is an expression of conservation of canonical angular momentum (see Section

Electric and Magnetic Field Lenses

7.4). It holds even when the assumptions of this calculation are not valid. Equation (6.23) implies that particles gain no net azimuthal velocity passing completely through the lens. This comes about because they must cross negatively directed radial magnetic field lines at the exit that cancel out the azimuthal velocity gained at the entrance. Recognizing that $d\theta/dt = v_\theta/r$ and assuming that B_z is approximately constant in r , the angular rotation of an orbit passing through the lens is

$$(\theta - \theta_o) = [qB_z(0,z)/2\gamma m_o v_z] (z - z_o). \quad (6.24)$$

Rotation is the same for all particles, independent of radius. Substituting Eq. (6.23) and converting the time derivative to a longitudinal derivative, Eq. (6.21) can be integrated to give

$$r_f' = \frac{v_{rf}}{v_z} \cong \frac{-\int dz [qB_z(0,z)/\gamma m_o v_z]^2 r}{4}. \quad (6.25)$$

The focal length for a solenoidal magnetic lens is

$$f = \frac{-r_f}{r_f'} = \frac{4}{\int dz [qB_z(0,z)/\gamma m_o v_z]^2}. \quad (6.26)$$

The quantity in brackets is the reciprocal of a gyroradius [Eq. (3.38)]. Focusing in the solenoidal lens (as in the immersion lens) is second order; the inward force results from a small azimuthal velocity crossed into the main component of magnetic field. Focusing power is inversely proportional to the square of the particle momentum. The magnetic field must increase proportional to the relativistic mass to maintain a constant lens power. Thus, solenoidal lenses are effective for focusing low-energy electron beams at moderate field levels but are seldom used for beams of ions or high-energy electrons.

6.8 MAGNETIC SECTOR LENS

The lenses of Sections 6.5-6.7 exert cylindrically symmetric forces via paraxial electric and magnetic fields. We now turn attention to devices in which focusing is one dimensional. In other words, if the plane perpendicular to the axis is resolved into appropriate Cartesian coordinates (x , y), the action of focusing forces is different and independent in each direction. The three examples we shall consider are (1) horizontal focusing in a sector magnet (Section 6.8), (2) vertical focusing at the edge of a sector magnet with an inclined boundary (Section 6.9), and (3) quadrupole field lenses (Section 6.10).

A sector magnet (Fig. 6.15) consists of a gap with uniform magnetic field extending over a bounded region. Focusing about an axis results from the location and shape of the field

Electric and Magnetic Field Lenses

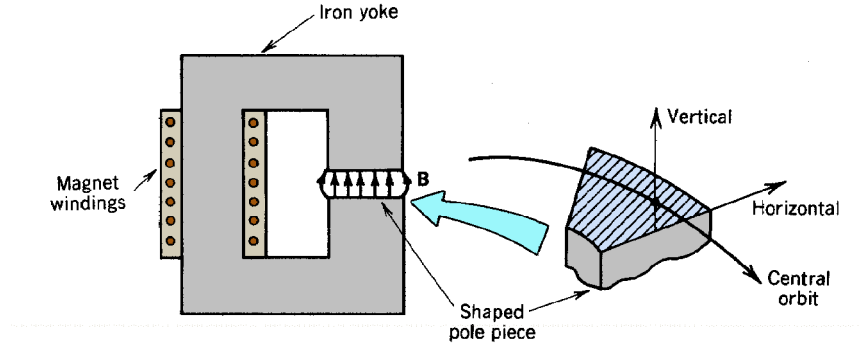


Figure 6.15 Sector field magnet for deflecting a beam showing definition of horizontal and vertical directions with respect to the main beam orbit.

boundaries rather than variations of the field properties. To first approximation, the field is uniform [$\mathbf{B} = B_x(x, y, z) \mathbf{x} = B_o \mathbf{x}$] inside the magnet and falls off sharply at the boundary. The x direction (parallel to the field lines) is usually referred to as the vertical direction. The y direction (perpendicular to the field lines) is the horizontal direction. The beam axis is curved. The axis corresponds to one possible particle orbit called the *central orbit*. The purpose of focusing devices is to confine non-ideal orbits about this line. Sector field magnets are used to bend beams in transport lines and circular accelerators and to separate particles according to momentum in charged particle spectrometers.

The 180° spectrograph (Fig. 6.16) is an easily visualized example of horizontal focusing in a sector field. Particles of different momentum enter the field through a slit and follow circular orbits with gyroradii proportional to momentum. Particles entering at an angle have a displaced orbit center. Circular orbits have the property that they reconverge after one half revolution with only a second-order error in position. The sector magnet focuses all particles of the same

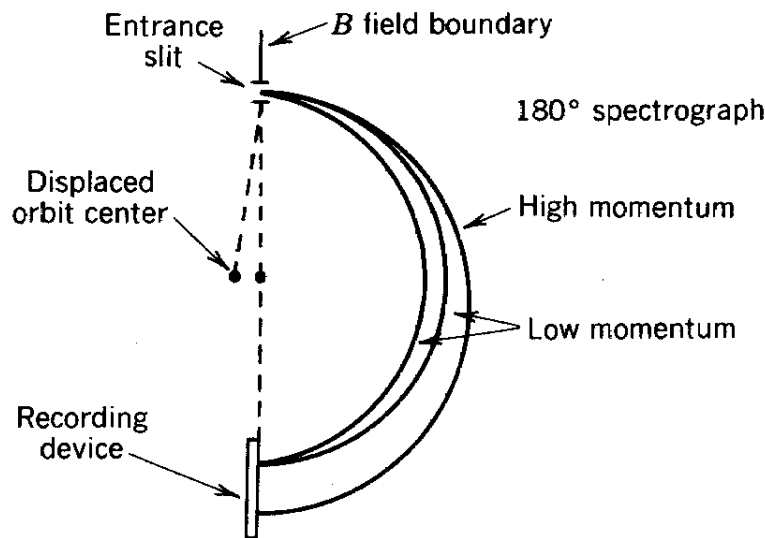


Figure 6.16 Particle focusing by a 180° sector magnet.

Electric and Magnetic Field Lenses

momentum to a line, independent of entrance angle. Focusing increases the acceptance of the spectrometer. A variety of entrance angles can be accepted without degrading the momentum resolution. The input beam need not be highly collimated so that the flux available for the measurement is maximized. There is no focusing in the vertical direction; a method for achieving simultaneous horizontal and vertical focusing is discussed in Section 6.9.

A sector field with angular extent less than 180° can act as a thick lens to produce a horizontal convergence of particle orbits after exiting the field. This effect is illustrated in Figure 6.17. Focusing occurs because off-axis particles travel different distances in the field and are bent a different amount. If the field boundaries are perpendicular to the central orbit, we can show, for initially parallel orbits, that the difference in bending is linearly proportional to the distance from the axis.

The orbit of a particle (initially parallel to the axis) displaced a distance Δr_i from the axis is shown in Figure 6.17. The final displacement is related by $\Delta y_f = \Delta y_i \cos \alpha$, where α is the angular extent of the sector. The particle emerges from the lens at an angle $\Delta \theta = -\Delta y_i \sin \alpha / r_g$, where r_g is the gyroradius in the field B_o . Given the final position and angle, the distance from the field boundary to the focal point is

$$f' = r_g / \tan \alpha. \quad (6.27)$$

The focal distance is positive for $\alpha < 90^\circ$; emerging particle orbits are convergent. It is zero at $\alpha = 90^\circ$; initially parallel particles are focused to a point at the exit of a 90° sector. At 180° the focusing distance approaches infinity.

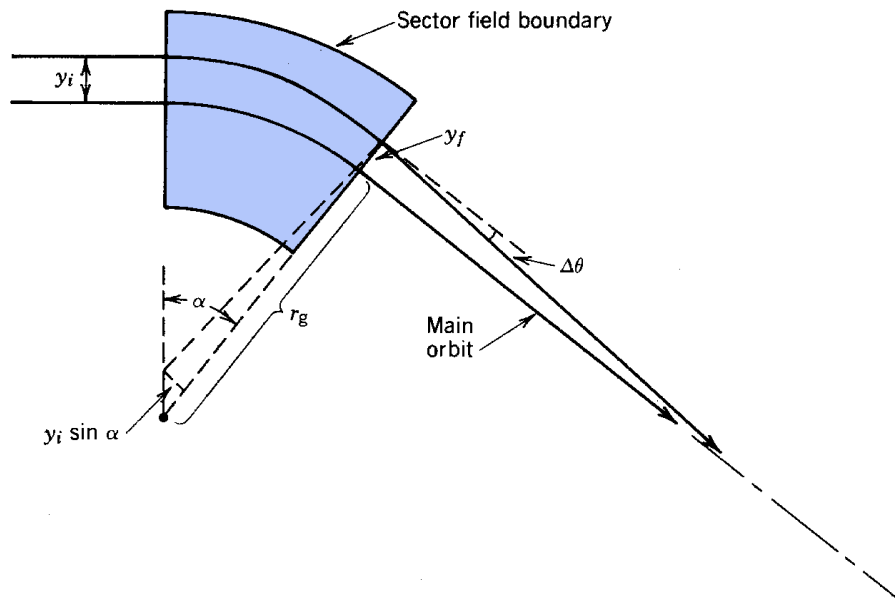


Figure 6.17 Geometry for calculating horizontal focal properties of a sector magnet.

Electric and Magnetic Field Lenses

The sector field magnet must usually be treated as a thick lens. This gives us an opportunity to reconsider the definition of the principal planes, which must be clarified when the beam axis is curved. The plane H_1 is the surface that gives the correct particle orbits in the image space. The appropriate construction is illustrated in Figure 6.18a. A line parallel to the beam axis in the image plane is projected backward. The principal plane is perpendicular to this line. The exit orbit intersects the plane at a distance equal to the entrance distance. If a parallel particle enters the sector field a distance y_i from the beam axis, its exit orbit is given by the line joining the focal point with a point on the principal plane y_i from the axis. The focal length is the distance from the principal plane to the focal point. The plane H_2 is defined with respect to orbits in the $-z$ direction.

The focal length of a sector can be varied by inclining the boundary with respect to the beam axis. Figure 18b shows a boundary with a positive inclination angle, β . When the inclination angle is negative, particles at a larger distance from the central orbit gyrocenter travel longer distances

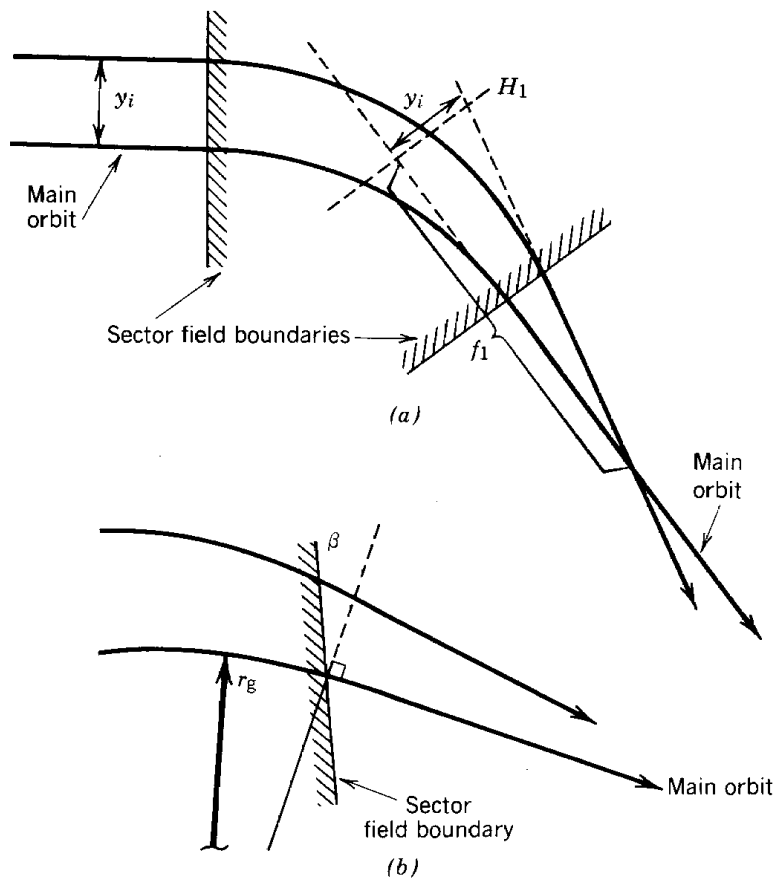


Figure 6.18 Focal properties of a sector magnet. (a) Definition of principal planes and focal lengths with a curved main orbit; thick-lens treatment of horizontal focusing in a sector magnet. (b) Effect on horizontal focusing of an inclination of the field boundary with respect to the main orbit.

Electric and Magnetic Field Lenses

in the field and are bent more. The focusing power of the lens in the horizontal direction is increased. Conversely, for $\beta > 0$, horizontal focusing is decreased. We will see in Section 6.9 that in this case there is vertical focusing by the fringing fields of the inclined boundary.

A geometric variant of the sector field is the toroidal field sector lens. This is shown in Figure 6.19. A number of magnet coils are arrayed about an axis to produce an azimuthal magnetic field. The fields in the spaces between coils are similar to sector fields. The field boundary is determined by the coils. It is assumed that there are enough coils so that the fields are almost symmetric in azimuth. The field is not radially uniform but varies as $B_\theta(R, Z) = B_o R_o / R$, where R is the distance from the lens axis. Nonetheless, boundaries can still be determined to focus particles to the lens axis; the boundaries are no longer straight lines. The figure shows a toroidal field sector lens designed to focus a parallel, annular beam of particles to a point.

The location of the focal point for a toroidal sector lens depends on the particle momentum. Spectrometers based on the toroidal fields are called *orange spectrometers* because of the resemblance of the coils to the sections of an orange when viewed from the axis. They have the advantage of an extremely large solid angle of acceptance and can be used for measurements at

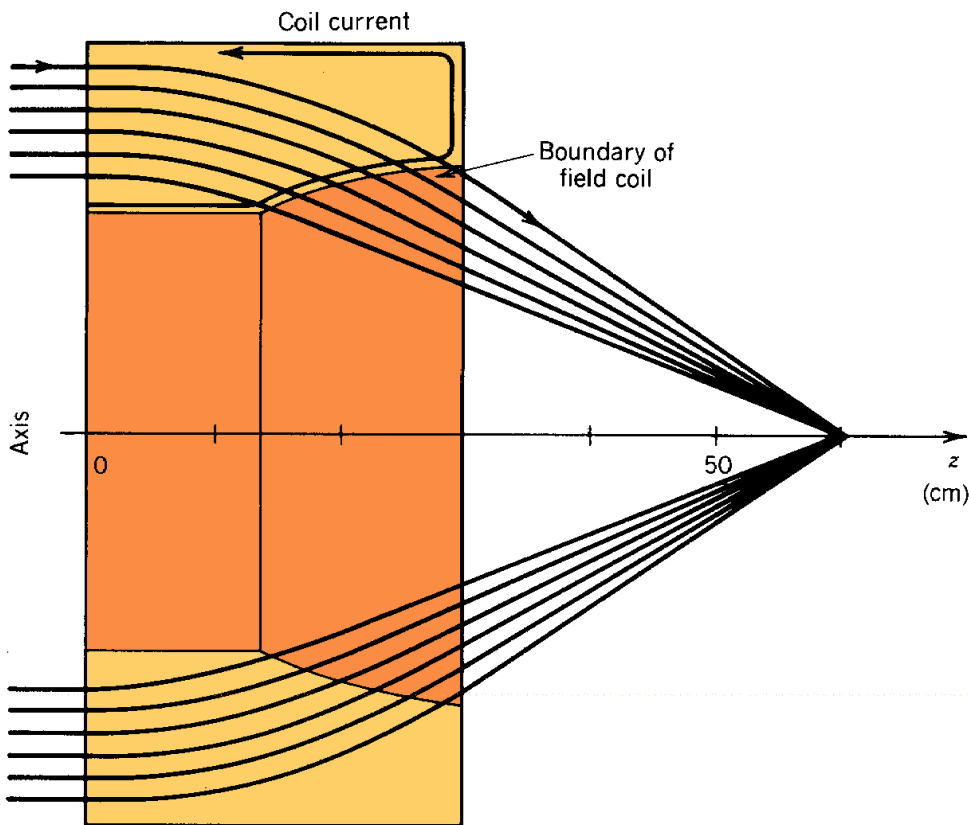


Figure 6.19 Particle orbits in a toroidal field lens with an exit boundary optimized for focusing an annular beam to a spot.

Electric and Magnetic Field Lenses

low flux levels. The large acceptance outweighs the disadvantage of particle loss on the coils.

The toroidal field sector lens illustrates the advantages gained by locating applied currents within the volume of the beam. The lens provides first-order focusing with cylindrical symmetry about an axis, as contrasted to the solenoidal field lens, which has second-order focusing. The ability to fine tune applied fields in the beam volume allows correction of focusing errors (aberrations) that are unavoidable in lenses with only external currents.

6.9 EDGE FOCUSING

The term edge focusing refers to the vertical forces exerted on charged particles at a sector magnet boundary that is inclined with respect to the main orbit. Figure 6.20 shows the fringing field pattern at the edge of a sector field. The vertical field magnitude decreases away from the magnet over a scale length comparable to the gap width. Fringing fields were neglected in treating perpendicular boundaries in Section 6.8. This is justified if the gap width is small compared to the particle gyroradius. In this case, the net horizontal deflection is about the same whether or not some field lines bulge out of the gap. With perpendicular boundaries, there is no force in the vertical direction because $B_y = 0$.

In analyzing the inclined boundary, the coordinate z is parallel to the beam axis, and the coordinate ξ is referenced to the sector boundary (Fig. 6.20). When the inclination angle β is nonzero, there is a component of \mathbf{B} in the y direction which produces a vertical force at the edge when crossed into the particle v_z . The focusing action can be calculated easily if the edge is treated as a thin lens; in other words, the edge forces are assumed to provide an impulse to the particles. The momentum change in the vertical direction is

$$\Delta P_x = \int dt (qv_z B_y). \quad (6.28)$$

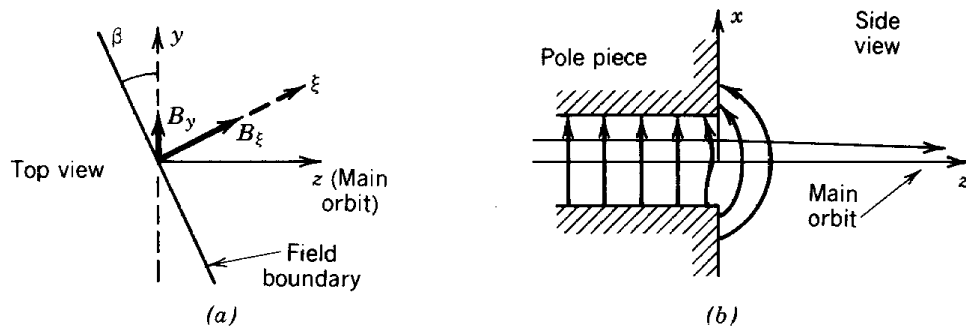


Figure 6.20 Geometry for calculating vertical focusing by a sector magnet boundary inclined with respect to the main orbit (edge focusing). (a) Field components at exit boundary, viewed along vertical direction (top view). (b) View of exit boundary along horizontal direction (side view).

Electric and Magnetic Field Lenses

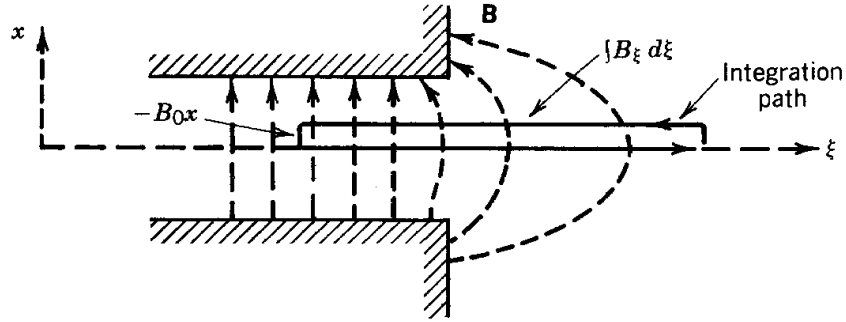


Figure 6.21 Geometry for evaluating field integral relevant to edge focusing.

The integral is taken over the time the particle is in the fringing field. The y component of magnetic field is related to the ξ component of the fringing field by $B_y = B_\xi \sin \beta$. The integral of Eq. (6.28) can be converted to an integral over the particle path noting that $v_z dt = dz$. Finally, the differential path element can be related to the incremental quantity $d\xi$ by $dz = d\xi / \cos \beta$. Equation (6.28) becomes

$$\Delta v_x = (e/\gamma m_o) \int d\xi B_\xi \tan \beta. \quad (6.29)$$

This integral can be evaluated by applying the equation $\oint \mathbf{B} \cdot d\mathbf{s} = 0$ to the geometry of Figure 6.21. The circuital integral extends from the uniform field region inside the sector magnet to the zero field region outside. This implies that $\int B_\xi d\xi = B_o x$. Substituting into Eq. (6.29), the vertical momentum change can be calculated. It is proportional to x , and the focal length can be determined in the usual manner as

$$f_x = \frac{\gamma m_o v_z / q B_o}{\tan \beta} = \frac{r_{go}}{\tan \beta}. \quad (6.30)$$

The quantity r_{go} is the particle gyroradius inside the constant-field sector magnet. When $\beta = 0$ (perpendicular boundary), there is no vertical focusing, as expected. When $\beta > 0$, there is vertical focusing, and the horizontal focusing is decreased. If β is positive and not too large, there can still be a positive horizontal focal length. In this case, the sector magnet can focus in both directions. This is the principal of the dual-focusing magnetic spectrometer, illustrated in Figure 6.22. Conditions for producing an image of a point source can be calculated using geometric arguments similar to those already used. Combined edge and sector focusing has also been used in a high-energy accelerator, the zero-gradient synchrotron [A. V. Crewe, *Proc. Intern. Conf. High Energy Accelerators*, CERN, Geneva, 1959, p. 359] (Section 15.5).

6. 10 MAGNETIC QUADRUPOLE LENS

The magnetic quadrupole field was introduced in Section 5.8. A quadrupole field lens is illustrated in Figure 5.16. It consists of a magnetic field produced by hyperbolically shaped pole pieces extending axially a length l . In terms of the transverse axes defined in Figure 5.161, the field components are $B_x = B_o y/a$ and $B_y = B_o x/a$. Because the transverse magnetic deflections are normal to the field components, $F_x \sim x$ and $F_y \sim y$. Motions in the transverse directions are independent, and the forces are linear. We can analyze motion in each direction separately, and we know (from Section 6.3) that the linear fields will act as one-dimensional focusing (or defocusing) lenses.

The orbit equations are

$$d^2y/dz^2 = (qB_o/\gamma m_o a v_z) y, \quad (6.31)$$

$$d^2x/dz^2 = -(qB_o/\gamma m_o a v_z) x. \quad (6.32)$$

The time derivatives were converted to axial derivatives. The solutions for the particle orbits are

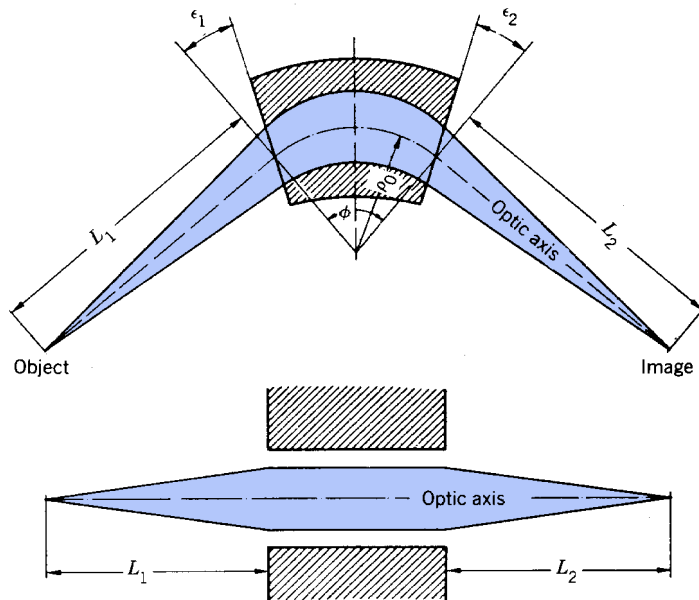


Figure 6.22 A homogeneous sector field in which the particle beam crosses the boundary obliquely. Proper choice of the angles ϵ_1 and ϵ_2 gives stigmatic focusing in both the radial and vertical directions. (Courtesy, H. Wollnik.)

Electric and Magnetic Field Lenses

$$x(z) = x_1 \cos\sqrt{\kappa_m}z + x_1' \sin\sqrt{\kappa_m}z / \sqrt{\kappa_m}, \quad (6.33)$$

$$x'(z) = -x_1 \sqrt{\kappa_m} \sin\sqrt{\kappa_m}z + x_1' \cos\sqrt{\kappa_m}z. \quad (6.34)$$

$$y(z) = y_1 \cos\sqrt{\kappa_m}z + y_1' \sin\sqrt{\kappa_m}z / \sqrt{\kappa_m}, \quad (6.35)$$

$$y'(z) = y_1 \sqrt{\kappa_m} \sin\sqrt{\kappa_m}z + y_1' \cos\sqrt{\kappa_m}z. \quad (6.36)$$

where $x_1, y_1, x_1',$ and y_1' are the initial positions and angles. The parameter κ_m is

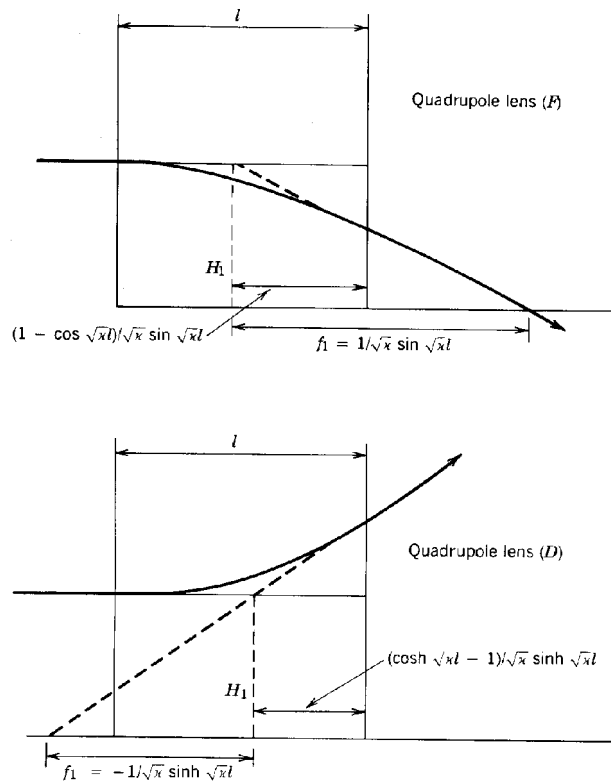


Figure 6.23 Principal planes and focal lengths for a magnetic quadrupole lens.

Electric and Magnetic Field Lenses

$$\kappa_m = qB_o/\gamma m_o a v_z \quad (m^{-2}) \quad (6.37)$$

where B_o is the magnetic field magnitude at the surface of the pole piece closest to the axis and a is the minimum distance from the axis to the pole surface. A similar expression applies to the electrostatic quadrupole lens

$$\kappa_e = qE_o/\gamma m_o a v_z^2. \quad (m^{-2}) \quad (6.38)$$

In the electrostatic case, the x and y axes are defined as in Figure 4.14.

The principal plane and focal length for a magnetic quadrupole lens are shown in Figure 6.23 for the x and y directions. They are determined from the orbit expressions of Eqs. (6.33) and (6.34). The lens acts symmetrically for particle motion in either the $+z$ or $-z$ directions. The lens focuses in the x direction but defocuses in the y direction. If the field coils are rotated 90° (exchanging North and South poles), there is focusing in y but defocusing in x . Quadrupole lenses are used extensively for beam transport applications. They must be used in combinations to focus a beam about the axis. Chapter 8 will show that the net effect of equal focusing and defocusing quadrupole lenses is focusing.